

COH FLUIDS AT UPPER-MANTLE CONDITIONS: AN EXPERIMENTAL STUDY ON VOLATILE SPECIATION AND MINERAL SOLUBILITY IN THE MS + COH SYSTEM

CARLA TIRABOSCHI

Dipartimento di Scienze della Terra "Ardito Desio", Università di Milano, Via Botticelli 23, 20133 Milano

INTRODUCTION

Fluids are involved in many geological processes from controlling the location and extent of melting at subduction zones to hydrothermal ore genesis, earthquake generation, and rock-forming processes.

Water is considered the most abundant volatile-bearing species at mantle conditions (*e.g.*, Poli & Schmidt, 2002; Manning, 2004) and, so far, the most extensive experimental work on the effect of volatiles on mantle relations have been conducted on systems in presence of an aqueous fluid (see review by Ulmer, 2001).

Although subduction-related fluids appear to be dominated by an aqueous component, composition of arc-magmas gases and metasomatized mantle-wedge peridotites suggest that carbon, stored in the altered oceanic crust, ophicarbonates and metasediments, is also recycled back into the mantle wedge, at least partially (*e.g.*, Bebout, 1995; Wallace, 2005). Carbon is retained in graphite/diamond and in carbonate phases, which are refractory and stable at very high pressure, as shown by experimental data (Molina & Poli, 2000; Dasgupta & Hirschmann, 2006; Poli *et al.*, 2009). Thermodynamic models (*e.g.*, Kerrick & Connolly, 1998; Gorman *et al.*, 2006) predict very small CO₂ fractions in COH fluid resulting from decarbonation processes, which only occur at low-*P* and high-*T* conditions. However, at top-of-the-slab conditions the effect of carbonate dissolution could have an important role in raising the concentration of carbon in high-pressure fluids (Caciagli & Manning, 2003).

Several experimental studies investigated the effect of H₂O (*e.g.*, Green, 1973; Konzett & Ulmer, 1999; Fumagalli & Poli, 2005) and CO₂ (*e.g.*, Eggler, 1975; Wyllie, 1977; Dasgupta & Hirschmann, 2007) on subsolidus and melting relations in peridotitic systems at upper-mantle conditions. However, only few works consider the effect of the simultaneous occurrence of H₂O and CO₂ or more in general, the influence of COH fluids (*i.e.*, fluids belonging to the system C-O-H) on peridotitic systems (*e.g.*, Olafsson & Eggler, 1983; Wallace & Green, 1988; Tumiati *et al.*, 2013). In particular, the speciation of the COH fluid in equilibrium with mantle minerals has been mainly estimated through thermodynamic modeling (*e.g.*, Poli *et al.*, 2009; Tumiati *et al.*, 2013), using equations of state of simple H₂O-non-polar gas systems (*e.g.*, H₂O-CO₂-CH₄), equations that do not consider the complexity related to dissolution processes (Liebscher, 2010, and references therein).

In this article, experimental data on COH fluid composition in the COH-only system and in the MS + COH system at *P* = 1-3 GPa and *T* = 700-1200 °C will be presented, considering the volatile speciation of the fluid and the solute content of COH fluids in equilibrium with mantle minerals, such as forsterite, enstatite, and magnesite. We performed rocking piston-cylinder experiments at the Laboratory of Experimental Petrology, Department of Earth Sciences, University of Milan (Italy). A rocking piston-cylinder apparatus was employed to avoid chemical segregation, typical of fluid saturated systems (Schmidt & Ulmer, 2004).

The experimental approach relies on two different techniques: *i*) analysis by means of quadrupole mass spectrometer (QMS) of the COH fluid from pierced run capsules to retrieve speciation of volatile components and *ii*) analysis of frozen COH fluid with laser-ablation inductively coupled plasma-mass spectrometry (LA-ICP-MS) to measure the amount of solutes (Kessel *et al.*, 2004).

COH VOLATILE SPECIATION IN THE COH AND MS + COH SYSTEMS

Experimental procedure

Oxalic acid dihydrate (OAD; $\text{H}_2\text{C}_2\text{O}_4 \cdot 2\text{H}_2\text{O}$) was chosen as fluid source to generate a 1:1 H_2O - CO_2 mixture. Volatile speciation experiments were conducted in the COH system considering four types of capsule geometry: *i*) single Au capsule loaded with OAD; *ii*) single Au capsule loaded with OAD and graphite; *iii*) single Au capsule loaded with OAD, graphite and an oxygen buffer (iron-wustite, hematite-magnetite or nickel-nickel oxide); *iv*) double capsules (Eugster & Skippen, 1967) loaded with OAD and graphite in the inner $\text{Au}_{50}\text{Pd}_{50}$ capsule, and nickel-nickel oxide (NNO) + H_2O in the outer Au capsule. The double capsule technique was also employed for another set of experiments, performed in the MS + COH system, with carbon-saturated COH fluids in equilibrium with a mixture of forsterite with minor enstatite (FoEn). In these runs oxalic acid dihydrate, graphite and FoEn were loaded in the inner capsule.

Experiments were carried out in a rocking piston-cylinder apparatus, at pressures from 1 to 3 GPa and temperatures from 800 to 1000 °C. To investigate the effect of packing materials on the speciation of the COH fluid we choose two different materials to embed the experimental capsule: *i*) MgO rods drilled to accommodate the capsule and MgO powder to fill the voids; *ii*) BN rods and powder, with MgO spacers at the top and the bottom of the assembly. A set of experiments in oven at $T = 250$ °C starting from OAD and OAD + graphite + iron-wustite buffer was also performed to investigate the thermal dissociation of oxalic acid dihydrate at low T and ambient pressure conditions.

Analytical technique

A capsule-piercing device connected to a quadrupole mass spectrometer was designed to retrieve the volatile speciation of COH fluids. The capsule-piercing device consists of two parts: *i*) an extraction vessel (reactor) and *ii*) an electric furnace where the vessel is allocated. The reactor, made with Teflon®, is composed of a base part, where the capsule is placed, and a top part, where a steel pointer is mounted. The capsule, placed horizontally and partially embedded in epoxy, is mounted on cross steel support, designed to oppose the rotation given by the steel pointer during the piercing. The reactor is connected to a QMS through a heated line to avoid condensation of water on the tubes.

The system was calibrated for quantitative analyses of H_2O , CO_2 , CH_4 , CO , H_2 and O_2 . For every mass/charge (m/z) channel 310 points were registered, one point every 5 seconds, for a total time of 1550 seconds. To determine the moles of the COH species an areal balance was performed, considering the total moles of fluid evolved, and a matrix that describes the species in terms of m/z channels. A weighted least-squares method, where weights take into account that the system has a heteroskedastic distribution of errors, was used owing to the different analytical uncertainties expected for different components. Monte Carlo simulations provided the propagation of errors for each species, corresponding to the analytical uncertainty.

Results and discussion

The performed experiments, together with the run products are presented in Table 1.

The experiments, performed at $T = 250$ °C starting from OAD, showed a good agreement with literature data from Morgan *et al.* (1992), with the only exception of a slightly lower H_2O content retrieved in our experiment. However, it is worth to note that Morgan *et al.* (1992) did not directly measured H_2O , which was estimated through mass balance calculation.

Experiments performed in single capsules with no oxygen buffer, starting from oxalic acid dihydrate and graphite did not allow reliable COH fluid volatile speciation analyses as the capsules were only filled by air.

The compositions of quenched COH fluids generated from oxalic acid dihydrate, graphite and different oxygen buffers were compared with the COH fluid speciation calculated through thermodynamic modeling (Perplex; Connolly, 1990). Results suggest that COH fluid speciation can diverge considerably compared to the thermodynamic model depending on the experimental strategy adopted. The packing material around the capsule seems to strongly control the speciation of COH fluids in single capsule experiments. In particular, BN imposes

reducing conditions on the COH fluid, favoring the formation of H₂O. On the other hand MgO shift the composition toward more oxidized terms.

Table 1 - Run table. OAD, oxalic acid dihydrate; G, graphite; IW, iron-wustite; HM, hematite-magnetite; NNO, nickel-nickel oxide; FoEn: forsterite + enstatite mix. *double capsule experiments

Run	P (GPa)	T (°C)	Starting material	Buffer	Assembly	Run time (h)	Run products
COH11	1·10 ⁻⁹	250	OAD	-	-	1	H ₂ O + CO ₂ + CO
FM1	1·10 ⁻⁹	250	OAD	-	-	2	H ₂ O + CO ₂ + CO
COH12	1·10 ⁻⁹	250	OAD + G	IW	-	1	H ₂ O + H ₂ + CO ₂
COH26	1	800	OAD + G	-	MgO	72	Only air
COH27	1	800	OAD + G	-	BN	72	Only air
COH14	1	800	OAD + G	IW	MgO	24	H ₂ O + CH ₄ + CO ₂
COH15	1	800	OAD + G	HM	MgO	22	CO ₂ + H ₂ O + CO
COH19	1	800	OAD + G	NNO	MgO	72	CO ₂ + CO
COH20	1	800	OAD + G	NNO	BN	72	H ₂ O + H ₂
COH18*	1	800	OAD + G	NNO	MgO	21	CO ₂ + H ₂ O
CM3*	1	800	OAD + G + FoEn	NNO	MgO	48	CO ₂ + H ₂ O + CO
COH25	1	900	OAD + G	-	MgO	24	Only air
COH28	1	900	OAD + G	-	BN	24	Only air
COH32	1	900	OAD + G	NNO	MgO	24	CO ₂
COH29	1	900	OAD + G	NNO	BN	24	Only air
COH30*	1	900	OAD + G	NNO	MgO	24	CO ₂ + H ₂ O + CO
CM7*	1	900	OAD + G + FoEn	NNO	MgO	21	CO ₂ + CO + H ₂ O
COH16	3	1000	OAD + G	NNO	MgO	24	CO ₂ + CO + H ₂ O

Double capsule experiments, buffered at NNO hydrogen fugacity conditions, provided similar COH volatile speciation compared to thermodynamic modeling for what concerned the COH-only system. However, in complex COH systems the presence of solutes seems to affect the volatile speciation of the fluid, shifting the composition toward more CO₂-rich terms and maintaining the plotted compositions on the graphite saturation surface (Fig. 1).

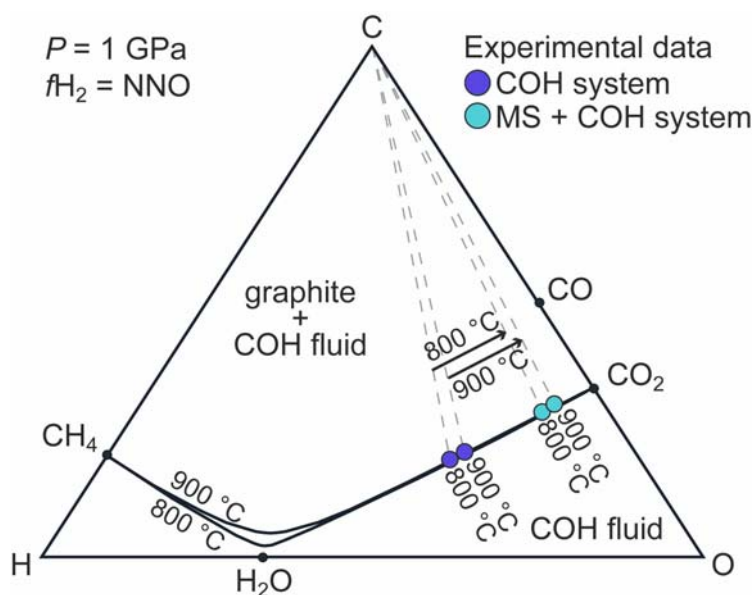


Fig. 1 - Composition of the COH fluid in the COH-only system and in the MS + COH from double capsules experiments plotted on the COH ternary diagram. Graphite saturation surfaces (black solid line) calculated by thermodynamic modeling.

With increasing temperature the experimental COH composition was more CO₂-rich, as predicted by the thermodynamic model and also observed in experiments in the COH-only system.

SOLUBILITY OF MANTLE MINERALS IN COH FLUIDS

Experimental procedure

To investigate the solubility of mantle minerals in COH fluids two starting materials were considered: *i*) a mixture of forsterite and minor enstatite (FoEn) and *ii*) a mixture of enstatite, magnesite and minor forsterite (EnMag). Carbon-saturated COH fluids were generated from oxalic acid anhydrous (OAA, H₂C₂O₄), H₂O, and graphite. A layer of diamond crystals with grain size of 20 μm was placed between two layers of the starting material to collect the fluid in equilibrium with solid phases. The thermal dissociation of OAA at high temperature generated a CO₂-H₂ 2:1 fluid. H₂O was added to obtain a roughly equimolar CO₂-H₂O 1:1 mixture in the capsule. Since the analytical technique (cryogenic laser-ablation ICP-MS technique; Kessel *et al.*, 2004) requires the use of an internal standard, to determine the amount of solutes trapped into the diamond layer, water was doped with 585 ppm of cesium (from CsOH) and its concentration was checked by means of ICP-MS. By knowing the initial Cs/H₂O ratio it is possible to retrieve the amount of solutes in the laser spot, since cesium is a highly incompatible element which is exclusively partitioned into the fluid phase.

All experimental runs were performed at fluid-saturated conditions, with fluid/solids ratio ~20 wt.%. Redox conditions were controlled employing the double capsule technique and nickel-nickel oxide buffer. The inner Au₅₀Pd₅₀ capsule was loaded with FoEn/EnMag, OAA, H₂O, graphite and diamonds. The outer capsule (Au at T < 1000 °C, Pt at T > 1000 °C) contains the inner capsule, the oxygen buffer NNO, and H₂O.

Experiments were carried out in a rocking piston-cylinder apparatus at pressures from 1 to 2.1 GPa and temperatures ranging from 700 to 1200 °C.

Analytical technique

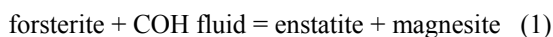
The solute content in the fluid was measured through the cryogenic laser-ablation ICP-MS technique also known as “freezing technique” (Kessel *et al.*, 2004). The recovered experimental capsule was mounted on a freezing stage, which consisted of a stack of two Peltier elements, surrounded by plastic to thermally insulate the elements from the atmosphere. The sample holder was placed on a copper block, in direct contact with Peltier elements and cooled to T = -35 °C. A longitudinal cross-section of the capsule was exposed using a cutter blade mounted on a steel support. The upper half of the capsule was removed and checked at the binocular microscope, whereas the lower part remained on the freezing stage for the laser ablation analyses and it remained frozen during the entire analytical session.

Analyses were performed at the Institute of Geological Sciences, University of Bern (Switzerland) using a 193 nm ArF GeoLas Pro excimer laser system coupled to an ELAN DRCD-e quadrupole mass spectrometer. The diamond trap for ²⁴Mg, ²⁵Mg, ²⁶Mg, ²⁹Si, ⁶²Ni, ¹³³Cs, ¹⁹⁵Pt, and ¹⁹⁷Au were analyzed using a 60 μm beam diameter and 5 Hz repetition rate. The concentration of the internal standard (Cs), corrected with a dilution model, was used to retrieve the amount of solutes in the fluid, as Cs fractionated completely into water. The use of a dilution model was necessary because the amount of water in the inner capsule was not constant and it was controlled by the nickel-nickel oxide buffer.

Capsules were also observed at the electron microscope (JEOL8200 Superprobe, University of Milan), to inspect the diamond trap and the eventual presence of precipitates in the diamond layer. WDS analyses and X-ray maps of elements were performed on the polished samples.

Results and discussion

At pressures ranging from 1 to 2.1 GPa and temperatures ranging from 700 to 1200 °C three phase assemblages were identified: *i*) forsterite + enstatite; *ii*) enstatite + magnesite; *iii*) talc + magnesite (Fig. 2). In Fig. 2 we also report the reaction:



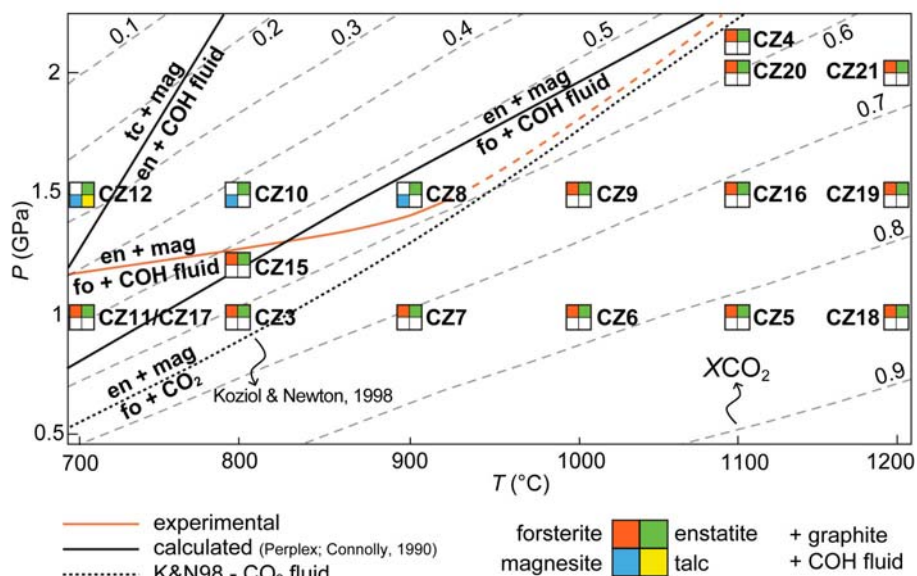


Fig. 2 - Phase assemblages in the MS + COH system buffered at $fH_2 = NNO$ conditions as a function of P and T. Reactions reported in black (solid lines) have been modeled with the software PerpleX (Connolly, 1990). Solid orange line represent the reaction forsterite + COH fluid = enstatite + magnesite based on the mineral assemblages observed in textural equilibrium. Dashed black line, reaction forsterite + CO₂ = enstatite + magnesite from Koziol & Newton (1998). Dashed gray lines represent XCO₂, estimated by thermodynamic modeling of a pure GCOH fluid externally buffered by nickel-nickel oxide.

Reaction 1 presented a weak pressure dependency and occurred at higher pressure compared to the carbonation reaction of forsterite determined by Koziol & Newton (1998) in the MS + CO₂ system. The shift toward higher pressures was predicted also by the calculated reaction through thermodynamic model and was caused by the presence of H₂O in the system. With increasing temperatures and molar fraction of CO₂, the experimental reaction approached that of Koziol & Newton (1998) as the composition of the fluid became more CO₂ rich.

The amount of SiO₂ and MgO in the aqueous fraction of the COH fluid expressed as molality ($m = \text{mol/kg}$) in equilibrium with forsterite + enstatite, enstatite + magnesite and talc + magnesite assemblages are reported in Table 2.

The SiO₂ content in the aqueous fraction of the COH fluid ranged from 0.74 mol/kg at (P = 1 GPa, T = 800 °C) to 4.02 mol/kg (P = 2 GPa, T = 1100 °C) for what concerned the forsterite + enstatite assemblage, whereas MgO ranged from 0.56 mol/kg (P = 1 GPa, T = 800 °C) to 5.01 mol/kg (P = 2 GPa, T = 1100 °C). The SiO₂ content in the aqueous fraction of the COH fluid, in equilibrium with enstatite and magnesite, spanned from 0.40 to 0.63 mol/kg and MgO from 0.35 to 0.63 mol/kg (P = 1.5 GPa, T = 800-900 °C). The $mSiO_2$ in the aqueous fraction of the COH fluid in equilibrium with talc + magnesite at P = 1.5 GPa and T = 700 °C was 1.52 mol/kg and $mMgO = 3.21 \text{ mol/kg}$.

The solute content in the COH fluid (Table 2) was retrieved by scaling the values of molality of SiO₂ and MgO to the amount of H₂O present in the COH fluid calculated by thermodynamic modeling. For what concerned the forsterite + enstatite assemblages, the SiO₂ content in the COH fluid ranged from 0.15 mol/kg (P = 1 GPa, T = 800 °C) to 1.57 mol/kg (P = 2 GPa, T = 1100 °C), whereas MgO spanned from 0.20 mol/kg (P = 1 GPa, T = 800 °C) to 1.95 mol/kg (P = 2 GPa, T = 1100 °C). The enstatite + magnesite assemblages presented the $mSiO_2$ ranging from 0.22 to 0.28 mol/kg and $mMgO$ from 0.20 to 0.28 mol/kg at P = 1.5 GPa and temperatures from 800 to 900 °C. The $mSiO_2$ in the reconstructed COH fluid in equilibrium with talc +

magnesite at $P = 1.5$ GPa and $T = 700$ °C was 0.96 mol/kg and $mMgO = 2.01$ mol/kg. In general we observed that pressure exerted a major role in raising the concentration of solutes in the COH fluid.

Table 2 - Solutes analyses in equilibrium with forsterite + enstatite, enstatite + magnesite and talc + magnesite assemblages. $mSiO_2$, $mMgO$ and $MgO + SiO_2$ refer to the aqueous part of the fluid.

Run	P (GPa)	T (°C)	Starting material	$mSiO_2$ (mol/kg)	$mMgO$ (mol/kg)	MgO + SiO_2 (wt.%)	$mSiO_2^*$ (mol/kg)	$mMgO^*$ (mol/kg)	MgO + SiO_2^* (wt.%)	XCO_2
<i>Forsterite + enstatite</i>										
CZ11	1	700	EnMag	0.91	0.12	5.61	0.48	0.06	2.95	0.47
CZ17	1	700	FoEn	0.74 (0.12)	0.56 (0.03)	6.30	0.39	0.29	3.31	0.47
CZ24	1	700	FoEn	0.45 (0.03)	0.27 (0.07)	3.55	-	-	-	-
CZ3	1	800	FoEn	0.49	0.67	5.37	0.19	0.26	2.05	0.62
CZ22	1	800	FoEn	0.28	0.30	2.80	-	-	-	-
CZ7	1	900	FoEn	1.45 (0.23)	0.60 (0.15)	10.0	0.42	0.17	2.92	0.71
CZ6	1	1000	FoEn	1.89 (0.95)	1.79 (0.63)	15.4	0.41	0.39	3.48	0.77
CZ5	1	1100	FoEn	2.63 (1.17)	4.22 (1.25)	24.4	0.44	0.70	4.40	0.82
CZ18	1	1200	FoEn	n.d.	n.d.	n.d.	n.d.	n.d.	n.d.	0.85
CZ15	1.2	800	EnMag	0.53 (0.09)	0.56 (0.06)	6.24	0.24	0.26	3.61	0.54
CZ9	1.5	1000	FoEn	2.30	3.47	21.8	0.79	1.19	7.61	0.65
CZ16	1.5	1100	FoEn	2.94 (0.57)	1.99 (0.45)	20.3	0.79	0.54	5.67	0.72
CZ19	1.5	1200	FoEn	n.d.	n.d.	n.d.	n.d.	n.d.	n.d.	0.77
CZ20	2	1100	FoEn	4.02 (0.97)	5.01 (1.77)	30.3	1.57	1.95	12.03	0.60
CZ21	2	1200	FoEn	n.d.	n.d.	n.d.	n.d.	n.d.	n.d.	0.67
CZ4	2.1	1100	FoEn	n.d.	n.d.	n.d.	n.d.	n.d.	n.d.	0.58
<i>Enstatite + magnesite</i>										
CZ10	1.5	800	EnMag	0.40 (0.02)	0.35 (0.09)	3.38	0.23	0.20	1.95	0.43
CZ8	1.5	900	FoEn	0.63 (0.32)	0.63 (0.24)	5.89	0.28	0.28	2.62	0.56
<i>Talc + magnesite</i>										
CZ12	1.5	700	EnMag	1.52	3.21	18.1	0.96	2.01	13.7	0.24

Number in parenthesis indicates absolute one standard deviation (1σ) of the average of analysis. Missing value in parenthesis indicate one shot in the diamond trap. $mSiO_2^*$, $mMgO^*$ and $MgO + SiO_2^*$ refer to the reconstructed COH fluid. XCO_2 has been estimated by thermodynamic modeling of a pure GCOH fluid at $fH_2 = NNO$. n.d. = not determined.

These results evidence that SiO_2 solubility in COH fluids is lower compared to experiments in the pure H_2O system and also compared to literature data (Nakamura & Kushiro, 1974; Manning & Boettcher, 1994; Zhang & Frantz, 2000; Newton & Manning, 2002) as shown in Fig. 3.

On the other hand, the presence of CO_2 seems to favor the formation of Mg-solutes (Fig. 3) compared to the estimated values of MgO solubility in the forsterite + enstatite + H_2O system (Zhang & Frantz, 2000).

GENERAL DISCUSSION AND CONCLUSIONS

Our experimental results in the COH and MS + COH systems at $P = 1$ GPa and $T = 700$ - 800 °C retrieved through the capsule-piercing QMS technique, suggest that the addition of forsterite + enstatite to the COH fluid shifts the volatile speciation toward CO_2 at fixed P-T- fH_2 conditions. At $P = 1$ GPa, data show an increase in XCO_2 ($= CO_2/H_2O + CO_2$) of + 45.8% at $T = 800$ °C and of + 50.5% at $T = 900$ °C in the COH fluid in equilibrium with forsterite + enstatite compared to a pure COH fluid. Although at this stage it is only possible to speculate about a process able to induce this difference, it appears evident that the increased amount of CO_2 is

related to an interaction of the COH fluid with solid phases, in particular with the assemblage forsterite + enstatite, which represents a model upper-mantle mineralogical composition.

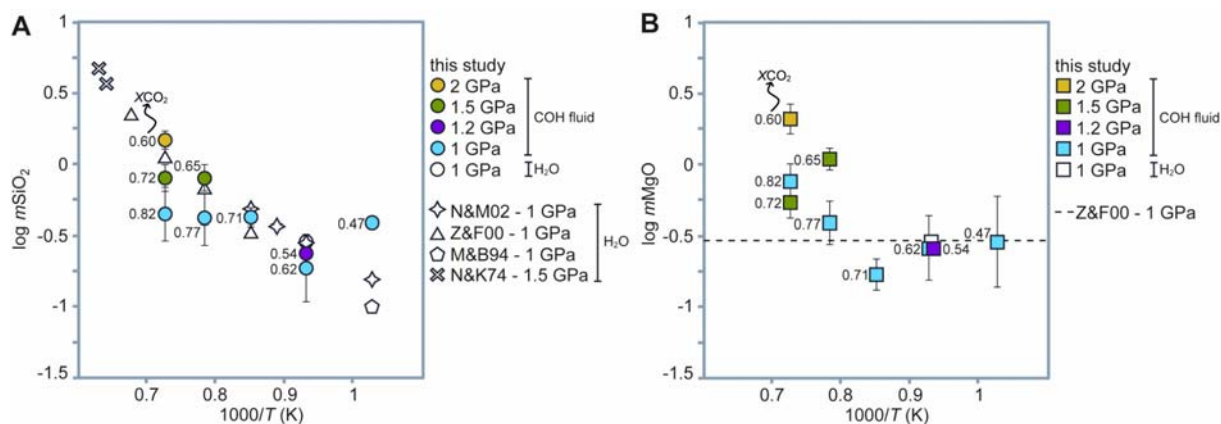
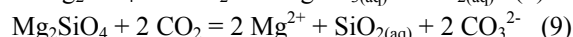
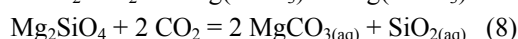
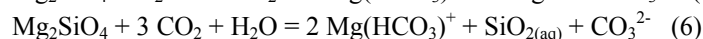
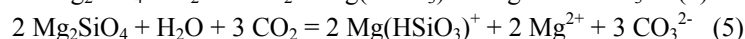
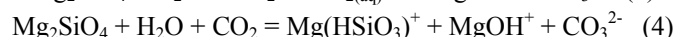
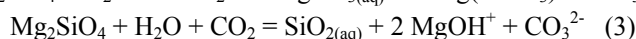
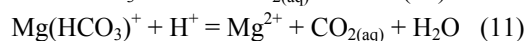


Fig. 3 - SiO₂ (A) and MgO (B) content in the reconstructed COH fluid and in pure H₂O in equilibrium with forsterite + enstatite assemblage. Experimental data from literature on forsterite + enstatite solubility in H₂O are also reported. N&K74, Nakamura & Kushiro (1974); M&B94, Manning & Boettcher (1994); Z&F00, Zhang & Frantz (2000); N&M02, Newton & Manning (2002). The dashed line represent the upper limit of MgO content in a H₂O fluid deriving from a forsterite + enstatite assemblage (Zhang & Frantz, 2000). Values near symbols are the correspondent XCO₂ of the fluid, estimated by thermodynamic modeling.

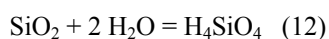
A series of possible dissolution reactions of forsterite, producing dissolved species containing carbon, such as CO₃²⁻ and Mg(HCO₃)⁺ are reported below:



These reactions will increase the amount of carbon in the fluid, but not in CO₂ species. In order to get the increase of CO₂ that we observed in our experiments, suggest the following reactions have been suggested, occurring in addition to reactions 2-9:



In reactions 10 and 11 CO_{2(aq)} occurs instead of carbonate species. Unlike carbonate species, CO_{2(aq)} can be exsolved at subsolvus P-T-X conditions, so these reactions could at least partially explain the observed increase in CO₂. The amount of CO_{2(aq)} is proportional to the amount of forsterite dissolved in the fluid. Following our data, this amount is 2-4 wt.% (SiO₂ + MgO) at P = 1 GPa and T = 800-1100 °C, and 12 wt.% at P = 2 GPa and T = 1100 °C. Moreover, according to Zotov & Keppler (2000), silica-dimer forming reactions are the following dehydration reactions:





Therefore, these reactions could also modify the composition of the COH fluid by increasing XCO₂.

In conclusion, dissolution processes of mantle minerals such as forsterite and enstatite, could contribute to increase the amount of CO₂ in high-pressure COH fluid. As a consequence, the total amount of CO₂ retained in COH fluids infiltrating the mantle-wedge could be remarkably high, and in any case much more compared to the quantities predicted by thermodynamic models in the simple COH system.

REFERENCES

- Bebout, G.E. (1995): The impact of subduction-zone metamorphism on mantle-ocean chemical cycling. *Chem. Geol.*, **126**, 191-218.
- Caciagli, N.C. & Manning, C.E. (2003): The solubility of calcite in water at 6-16 kbar and 500-800 °C. *Contrib. Mineral. Petr.*, **146**, 275-285.
- Connolly, J.A.D. (1990): Multivariable phase diagrams; an algorithm based on generalized thermodynamics. *Am. J. Sci.*, **290**, 666-718.
- Dasgupta, R. & Hirschmann, M.M. (2006): Melting in the Earth's deep upper mantle caused by carbon dioxide. *Nature*, **440**, 659-662.
- Dasgupta, R. & Hirschmann, M.M. (2007): Effect of variable carbonate concentration on the solidus of mantle peridotite. *Am. Mineral.*, **92**, 370-379.
- Eggler, D.H. (1975): Peridotite-carbonate relations in the system CaO-MgO-SiO₂-CO₂. *Carnegie Inst. Washington*, **74**, 468-474.
- Eugster, H.P. & Skippen, G.B. (1967): Igneous and metamorphic reactions involving gas equilibria. *Res. Geochem.*, **2**, 492-520.
- Fumagalli, P. & Poli, S. (2005): Experimentally determined phase relations in hydrous peridotites to 6.5 GPa and their consequences on the dynamics of subduction zones. *J. Petrol.*, **46**, 555-578.
- Gorman, P.J., Kerrick, D.M., Connolly, J.A.D. (2006): Modeling open system metamorphic decarbonation of subducting slabs. *Geochem. Geophys. Geosyst.*, **7**, doi:10.1029/2005GC001125.
- Green, D.H. (1973): Experimental melting studies on a model upper mantle composition at high pressure under water-saturated and water-undersaturated conditions. *Earth Planet. Sci. Letter*, **19**, 37-53.
- Kerrick, D.M. & Connolly, J.A.D. (1998): Subduction of ophicarbonates and recycling of CO₂ and H₂O. *Geology*, **26**, 375-378.
- Kessel, R., Ulmer, P., Pettke, T., Schmidt, M.W., Thompson, A.B. (2004): A novel approach to determine high-pressure high-temperature fluid and melt compositions using diamond-trap experiments. *Am. Mineral.*, **89**, 1078-1086.
- Konzett, J. & Ulmer, P. (1999): The stability of hydrous potassic phases in lherzolitic mantle. An experimental study to 9.5 GPa in simplified and natural bulk compositions. *J. Petrol.*, **40**, 629-652.
- Kozioł, A.M. & Newton, R.C. (1998): Experimental determination of the reaction: Magnesite + enstatite = forsterite + CO₂ in the ranges 6-25 kbar and 700-1100 °C. *Am. Mineral.*, **83**, 213-219.
- Liebscher, A. (2010): Aqueous fluids at elevated pressure and temperature. *Geofluids*, **10**, 3-19.
- Manning, C.E. (2004): The chemistry of subduction-zone fluids. *Earth Planet. Sci. Letter*, **223**, 1-16.
- Manning, C.E. & Boettcher, S.L. (1994): Rapid-quench hydrothermal experiments at mantle pressures and temperatures. *Am. Mineral.*, **79**, 1153-1158.
- Molina, J.F. & Poli, S. (2000): Carbonate stability and fluid composition in subducted oceanic crust: an experimental study on H₂O-CO₂-bearing basalts. *Earth Planet. Sci. Letter*, **176**, 295-310.
- Morgan, G.B., Chou, I., Pasteris, J.D. (1992): Speciation in experimental COH fluids produced by the thermal dissociation of oxalic acid dihydrate. *Geochim. Cosmochim. Acta*, **56**, 281-294.
- Nakamura, Y. & Kushiro, I. (1974): Composition of the gas phase in Mg₂SiO₄-SiO₂-H₂O at 15 kbar. *Carnegie Inst. Washington*, **73**, 255-258.
- Newton, R.C. & Manning, C.E. (2002): Solubility of enstatite + forsterite in H₂O at deep crust/upper mantle conditions: 4 to 15 kbar and 700 to 900 °C. *Geochim. Cosmochim. Acta*, **66**, 4165-4176.
- Olafsson, M. & Eggler, D.H. (1983): Phase relations of amphibole, amphibole-carbonate, and phlogopite-carbonate peridotite: petrologic constraints on the asthenosphere. *Earth Planet. Sci. Letter*, **64**, 305-315.
- Poli, S. & Schmidt, M.W. (2002): Petrology of subducted slabs. *Ann. Rev. Earth Planet. Sci.*, **30**, 207-235.

- Poli, S., Franzolin, E., Fumagalli, P., Crottini, A. (2009): The transport of carbon and hydrogen in subducted oceanic crust: an experimental study to 5 GPa. *Earth Planet. Sci. Letter*, **278**, 350-360.
- Schmidt, M.W. & Ulmer, P. (2004): A rocking multianvil: elimination of chemical segregation in fluid-saturated high-pressure experiments. *Geochim. Cosmochim. Acta*, **68**, 1889-1899.
- Tumiati, S., Fumagalli, P., Tiraboschi, C., Poli, S. (2013): An Experimental Study on COH-bearing Peridotite up to 3.2 GPa and Implications for Crust-Mantle Recycling. *J. Petrol.*, **54**, 453-479.
- Ulmer, P. (2001): Partial melting in the mantle wedge - the role of H₂O in the genesis of mantle-derived 'arc-related' magmas. *Phys. Earth Planet. Inter.*, **127**, 215-232.
- Wallace, M.E. & Green, D.H. (1988): An experimental determination of primary carbonatite magma composition. *Nature*, **335**, 343-346.
- Wallace, P.J. (2005): Volatiles in subduction zone magmas: concentrations and fluxes based on melt inclusion and volcanic gas data. *J. Volcanol. Geoth. Res.*, **140**, 217-240.
- Wyllie, P.J. (1977): Effects of H₂O and CO₂ on magma generation in the crust and mantle. *J. Geol. Soc. London*, **134**, 215-234.
- Zhang, Y.G. & Frantz, J.D. (2000): Enstatite-forsterite-water equilibria at elevated temperatures and pressures. *Am. Mineral.*, **85**, 918-925.
- Zotov, N. & Keppler, H. (2000): In-situ Raman spectra of dissolved silica species in aqueous fluids to 900 °C and 14 kbar. *Am. Mineral.*, **85**, 600-604.